IEEE Access
Multidisciplinary : Rapid Review : Open Access Journal

Received February 22, 2020, accepted March 22, 2020, date of publication March 26, 2020, date of current version April 15, 2020.

Digital Object Identifier 10.1109/ACCESS.2020.2983454

Adaptive Iterative Learning Control for Tank Gun Servo Systems With Input Deadzone

YUNTAO ZHANG[1], QIUZHEN YAN[1], JIANPING CAI[2], AND XIUSHAN WU[2]
[1]College of Information Engineering, Zhejiang University of Water Resources and Electric Power, Hangzhou 310018, China
[2]School of Electrical Engineering, Zhejiang University of Water Resources and Electric Power, Hangzhou 310018, China

Corresponding author: Yuntao Zhang (zhangyuntaozj@sina.com)

This work was part supported in part by the National Natural Science Foundation of China under Grant NSFC: 61573322, and in part by the Scientific Research Project of the Water Conservancy Department of Zhejiang Province under Grant RC1858.

ABSTRACT In this paper, an adaptive iterative learning control scheme is proposed to solve the trajectory-tracking problem for tank gun servo systems with input deadzone and arbitrary initial states. A time-varying boundary layer is constructed to deal with the nonzero initial error during the iterative learning controller design. Neural network control and robust control are jointly used to compensate uncertainties and deadzone nonlinearity. The ideal weight of neural network and the upper bound of noncontinuous uncertainties are estimated by using difference learning method. As the iteration number increases, the filtering error can converge to the time-varying boundary layer. All signal are guaranteed to be bounded. A simulation example is presented to verify the effectiveness of the proposed scheme.

INDEX TERMS Tank gun servo systems, iterative learning control, deadzone.

I. INTRODUCTION

Tank is a useful weapon in battle fields, whose effects include helping troops enhance the efficiency of artillery firepower and improving the surviving ability of soldiers. During fighting situations, the tank gun control servo systems are required to accomplish missions with accuracy, stability and speed of response, despite the existence of friction, uncertainties and external disturbances. Researchers have explored the motion control of tank gun servo systems for at least three decades. Dana *et al.* proposed a variable structure control scheme to solve the position trajectory tracking problem for uncertain tank gun systems [1]. In [2] and [3], optimal control technique was adopted to control design for tanks. In [4], a PID control algorithm was proposed to realize the firing precise control for tanks in motion. For compensating uncertainties and external disturbances in tank gun servo systems, adaptive control and its related control technology were adopted to the motion control, such as direct adaptive control [5], adaptive fuzzy control [6] and adaptive robust control [7]. The corresponding strategies of disturbance observer were reported in [8] and [9], respectively. In [10], the adaptive neural network was used to approximate the uncertainties and disturbances in tank gun servo control systems. In [11], an event-triggered adaptive control scheme was proposed for the gun control system subjected to external disturbances, uncertain modeling errors and unknown parameters. In [12], an adaptive learning control scheme was proposed to solve high-precision velocity tracking problem for tank gun control servo systems under alignment condition. These above results have promoted the development of control technique for tank gun servo control systems. However, due to the inaccurate system modeling and complex working environments, how to obtain good control performance for the tank gun servo systems has been not easily accomplished.

The associate editor coordinating the review of this manuscript and approving it for publication was Chao-Yang Chen.

The past decades have witnessed the great efforts to investigate advanced industry control schemes for obtaining better control performance [43]. As a well-known high-precision control technique, iterative learning control (ILC) is effective in dealing with repeated control processes over a finite interval [13]–[17]. One of its merits is that ILC can work well in the cases where the system model is hard to be got. In an ILC system, through updating the control input according to system error and the system operation information in the previous iteration, the tracking performances may be gradually improved, until perfect tracking performance may be obtained after many iterations. Up to now, there have been many ILC results on the position/velocity control of motors [18], [19]. In [20], an ILC scheme was proposed to reduce periodic torque pulsations in permanent magnet synchronous motors. The motion control of permanent magnet synchronous motors was considered in [21], where ILC technique was used to eliminate the influence of force ripple on the system performance of a position servo system. In [22], Precup *et al.* proposed a 2-DOF proportional-integral-fuzzy control scheme for a class of servo systems, in which, an iterative feedback tuning strategy is adopted to achieve the extended symmetrical optimum control design. On the whole, the ILC results on the trajectory-tracking problem for gun control servo systems of tank is few.

We consider two important aspects of ILC algorithm designs for tank gun servo systems in this work. The first aspect is about the initial state condition of ILC. In most existing ILC schemes, the initial system error is required to be zero at each iteration [23]–[25]. Otherwise, a slight initial error may lead to divergence of the tracking error. Since perfect system resetting for each iteration is not easily achievable in actual applications, relaxing or removing the zero-error resetting condition is of practical significance for ILC design. Adaptive ILC without zero-error resetting condition has been explored in this decade, and a few solutions have been proposed such as time-varying boundary layer technique [26], error-tracking method [27]–[29], initial rectifying action [30]–[32] and so on. Up to now, the ILC results on accurate tracking for tank gun control servo systems have been very few yet.

The second aspect we will address in this work is about the compensation of deadzone nonlinearities. In the actuator of motion control, there often exist nonlinearities such as saturation, deadzone and hysteresis. Since these nonlinearities degrade the control performance, the corresponding compensating should be adopted for improving control performance in the process of controller design. Among saturation, deadzone and hysteresis, deadzone is a class of the most common nonlinearities [33]. Up to now, there have been three strategies to deal with deadzone nonlinearities. The first one is direct adaptive compensating approach [34], [35]. In this approach, the parameters of deadzone are estimated by constructing an adaptive deadzone inverse model. Robust adaptive compensating approach is an alternative approach [36], [37]. In this approach, a deadzone nonlinearity is seen as the synthesis of a linear parametric uncertain term and a disturbance, which may be respectively compensated according to adaptive control technique and robust control technique. The third one is to approximate deadzone by using neural networks [38] or fuzzy systems [39]. So far, the research resluts on the tank gun servo systems with input deadzone have been very few [40]. To the best of authors' knowledge, the adaptive ILC for tank gun servo systems with arbitrary initial states and input deadzone has not been investigated yet, which motivates the current study of this paper.

This paper focus the adaptive ILC algorithm design for tank gun servo systems with arbitrary initial states and input deadzone. The time-varying boundary layer method is adopted to deal with the nonzero initial errors in tank gun servo systems. Neural network control technique, together with robust control technique, is used to deal with uncertainties and deadzone nonlinearity. It is shown that the velocity trajectory of tank gun servo systems can accurately track the desired signal by the proposed ILC control scheme. Comparing with existing results, the main contributions of this work lie in the following:

(1) Time-varying boundary layer approach is adopted to deal with the nonzero initial error problem in the ILC design for tank gun servo systems.

(2) Through constructing a proper Lyapunov function, an adaptive ILC scheme is proposed for tank gun servo control systems with the input deadzone.

(3) Adaptive learning neural network and robust control are adopted to compensate the uncertainties , disturbance end deadzone nonlinearities in tank gun servo systems.

The rest of this paper is organized as follows. The problem formulation is introduced in Section 2. The detailed design process of ILC system is addresed in Section 3. Section 4 presents the convergence analysis of the closed loop tank gun servo system. To demonstrate the effectiveness of the proposed adaptive ILC scheme, an illustrated example is shown in Section 5, followed by Section 6 which concludes this work.

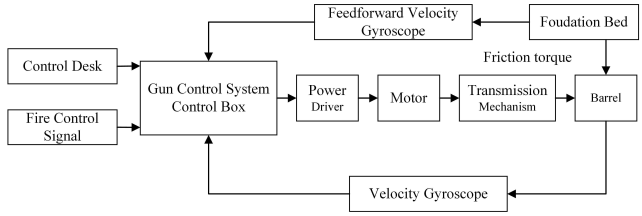

FIGURE 1. Structure diagram of vertical servo system of all-electrical tank gun.

II. PROBLEM FORMULATION

In all-electric tank gun control systems, the horizontal-direction adjustments and vertical-direction adjustments of turret and gun are accomplished by motor drives. Due to the advantages such as simple structure, excellent performance and high efficiency, nowadays full-electric tank gun control systems have been widely adopted as a replacement for traditional electro-hydraulic/all-hydraulic gun control systems. The structure diagram of vertical servo system of all-electrical tank gun is shown in Fig. 1. It can be seen that the controlled device mainly includes AC motor, speed reducer and barrel.

The block diagram of tank gun control systems, a careful reduction of a complex nonlinear simulation model, is shown in Fig. 2. The definition of corresponding variables and parameters in this figure is presented in Table 1.

On the basis of Fig. 2, we can get the model of gun control servo systems of tank as

$$\dot{i}_q = -\frac{R}{L}i_q - \frac{K_e i}{L}\omega + \frac{K_a}{L}u_q, \tag{1}$$

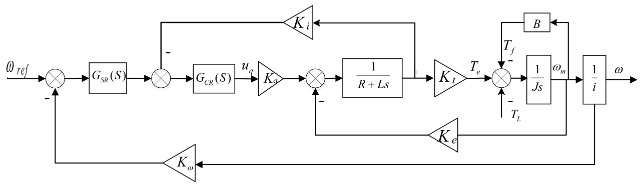

FIGURE 2. Block diagram of tank gun control systems.

TABLE 1. The definitions of symbols.

Symbol	Definition
ω_{ref}	desired angular velocity of cannon
ω	real angular velocity of cannon
$G_{CR}(s)$	velocity regulator
$G_{CR}(s)$	current regulator
R	resistance of the motor armature circuit
L	inductance of the motor armature circuit
K_a	amplifier gain
E_a	armature back electromotive force of motor
K_i	current feedback coefficient of q axis
E_a	armature back electromotive force of motor
K_e	electric torque coefficient
T_e	motor torque
T_L	load torque disturbance
T_f	friction torque disturbance
T_e	motor torque
T_L	load torque disturbance
T_f	friction torque disturbance
K_ω	angular velocity feedback coefficient of cannon
J	total moment of inertia to the rotor
B	viscous friction coefficient
i	moderating ratio
s	Laplace operator

$$\dot{\omega} = \frac{K_t}{Ji} i_q - \frac{1}{Ji} T_{Ls}, \tag{2}$$

where $T_{Ls} = T_L + T_f$. u_q and v are the input and the output of an unknown deadzone nonlinearity, and they meet the relationship as

$$u_q = \begin{cases} m_r(v - b_r) & v \geq b_r \\ 0 & b_l \leq v < b_r \\ m_l(v - b_l) & v < b_l, \end{cases} \tag{3}$$

where $m_r = m_l = m > 0$, $b_r > 0$, $b_l < 0$; the deadzone parameters including m, b_r and b_l are unknown; u_q is not available for measurement.

By letting

$$b_u = \begin{cases} b_r & v \geq b_r \\ u_q & b_l \leq v < b_r \\ b_l & v < b_l, \end{cases} \tag{4}$$

(3) can be rewritten as $u_q = v - b_u$. According to this, combining (1) with (2) yields

$$\ddot{\omega} = -\frac{R}{L}\dot{\omega} - \frac{K_t K_e}{LJ}\omega + \frac{K_a K_t}{LJi} m(v - b_u) - (\frac{R}{LJi} T_{Ls} + \frac{1}{Ji}\dot{T}_{Ls}).$$

Define $x_1 = \omega$, $x_2 = \dot{\omega}$. Then, from (5), the dynamics of tank gun control systems at the kth iteration can be written as

$$\begin{cases} \dot{x}_{1,k} = x_{2,k}, \\ \dot{x}_{2,k} = -\dfrac{R}{L} x_{2,k} - \dfrac{K_t K_e}{LJ} x_{1,k} + \dfrac{K_a K_t m}{LJi} v_k \\ -m b_u + \Delta f(\boldsymbol{x}_k, t), \end{cases} \tag{5}$$

where, $k \in N$ denotes the iteration number, $\boldsymbol{x}_k = [x_{1,k}, x_{2,k}]^T$, $\Delta f(\boldsymbol{x}_k, t) = -(\frac{R}{LJi} T_{Ls} + \frac{1}{Ji}\dot{T}_{Ls})$. Without loss of generality, we assume $\Delta f(\boldsymbol{x}_k, t) = f_1(\boldsymbol{x}_k) + f_2(\boldsymbol{x}_k, t)$, where $f_1(\boldsymbol{x}_k)$ represents a Liphitz continuous function with respect to $\boldsymbol{x}_k$, and $f_2(\boldsymbol{x}_k, t)$ represents noncontinuous but bounded perturbations. $|f_2(\boldsymbol{x}_k, t)| \leq \epsilon_f(t)$. $\epsilon_f(t)$ is an unknown time-varying but iteration-invariant parameter.

The control target is to find a sequence of appropriate control inputs v_k, such that as the learning number increases, $\boldsymbol{x}_k(t)$ can accurately track $\boldsymbol{x}_d(t)$ under the condition that $x_k(0) \neq \boldsymbol{x}_d(0)$.

III. CONTROL SYSTEM DESIGN

Based on (5), setting $\boldsymbol{e}_k(t) = [e_{1,k}(t), e_{2,k}(t)]^T = \boldsymbol{x}_k(t) - \boldsymbol{x}_d(t)$ leads to

$$\begin{cases} \dot{e}_{1,k} = e_{2,k}, \\ \dot{e}_{2,k} = -\dfrac{R}{L} x_{2,k} - \dfrac{K_t K_p}{LJ} x_{1,k} + \dfrac{K_a K_t m}{LJi} v_k \\ \quad -m b_u + \Delta f(\boldsymbol{x}_k, t) - \ddot{x}_d. \end{cases} \tag{6}$$

Let us define $s_k = \lambda e_{1,k} + e_{2,k}$, and

$$s_{\phi,k}(t) = s_k(t) - \phi_k(t)\mathrm{sat}_{-1,1}\left(\frac{s_k(t)}{\phi_k(t)}\right), \tag{7}$$

where,

$$\phi_k(t) = |s_k(0)| \mathrm{e}^{-\mu t}, \tag{8}$$

$\lambda > 0$, $\mu > 0$. The saturation function $\mathrm{sat}_{\cdot,\cdot}(\cdot)$ is defined as follows: for a scalar $\hat{a}$,

$$\mathrm{sat}_{\underline{a},\bar{a}}(\hat{a}) = \begin{cases} \bar{a} & \hat{a} > \bar{a} \\ \hat{a} & \underline{a} \leq \hat{a} \leq \bar{a} \\ \underline{a} & \hat{a} < \underline{a}; \end{cases}$$

for a vector $\hat{\boldsymbol{a}} = [\hat{a}_1, \hat{a}_2, \cdots, \hat{a}_m] \in \boldsymbol{R}^m$, $\mathrm{sat}_{\underline{a},\bar{a}}(\hat{\boldsymbol{a}}) = \left[\mathrm{sat}_{\underline{a},\bar{a}}(\hat{a}_1), \mathrm{sat}_{\underline{a},\bar{a}}(\hat{a}_2), \cdots, \mathrm{sat}_{\underline{a},\bar{a}}(\hat{a}_m)\right]^T$.

Remark 1: $\phi_k(t)$ is a time-varying boundary layer, whose absolute value decreases along time axis. Note that $s_{\phi,k}(0) = 0, \forall k$ holds, which helps to solve the initial problem of ILC.

Then, we choose a candidate control Lyapunov function at the kth iteration as

$$V_k = \frac{1}{2\beta} s_{\phi,k}^2, \tag{9}$$

where $\beta = \frac{K_a K_t m}{LJi}$. The time derivative of V_k is

$$\dot{V}_k = s_{\phi,k}[\frac{1}{\beta}(\lambda e_{2,k} - \frac{R}{L}x_{2,k} - \frac{K_t K_p}{LJ}x_{1,k} + f_1(\boldsymbol{x}_k) - \ddot{x}_d) + \frac{1}{\beta}(f_2(\boldsymbol{x}_k, t) - mb_u) + v_k] \tag{10}$$

$$= s_{\phi,k}[\boldsymbol{\theta}^T \boldsymbol{\psi}_k + \frac{1}{\beta}f_1(\boldsymbol{x}_k) + \frac{1}{\beta}(f_2(\boldsymbol{x}_k, t) - mb_u) + v_k], \tag{11}$$

where, $\boldsymbol{\theta} = [\frac{\lambda}{\beta}, -\frac{B}{L\beta}, -\frac{K_t K_p}{LJ\beta}, -\frac{1}{\beta}]^T$, $\boldsymbol{\psi}_k = [e_{2,k}, x_{2,k}, x_{1,k}, \ddot{x}_d]^T$. Then, a radial basis function (RBF) neural network is used to approximate $\frac{1}{\beta}f_1(\boldsymbol{x}_k)$, i.e.,

$$\frac{1}{\beta}f_1(\boldsymbol{x}_k) = \boldsymbol{\eta}^{*T}\boldsymbol{\varphi}(\boldsymbol{x}_k) + \epsilon(\boldsymbol{x}_k), \tag{12}$$

where $\boldsymbol{\eta}^*(t)$ is the ideal weight of neural network, $\epsilon(\boldsymbol{x}_k)$ is the approximation error of neural network, $|\epsilon(\boldsymbol{x}_k)| \le \epsilon_N$, and $\boldsymbol{\varphi}(\boldsymbol{x}_k) = [\varphi_{1,k}, \varphi_{2,k}, \cdots, \varphi_{m,k}]^T$ with

$$\varphi_{j,k} = \mathrm{e}^{-\frac{\|\boldsymbol{x}_k - \boldsymbol{c}_j\|^2}{2b_j^2}}, \quad j = 1, 2, \cdots, m. \tag{13}$$

In (13), $\boldsymbol{c}_j = [c_{j1}, c_{j2}]^T$ and b_j are the center vector and the width of the hidden layer, respectively.

Substituting (12) into (11), we have

$$\dot{V}_k = s_{\phi,k}[\boldsymbol{\theta}^T \boldsymbol{\psi}_k + \boldsymbol{\eta}^{*T}\boldsymbol{\varphi}(\boldsymbol{x}_k) + \epsilon(\boldsymbol{x}_k) + \frac{1}{\beta}(f_2(\boldsymbol{x}_k, t) - mb_u) + v_k]$$

$$\le s_{\phi,k}[\boldsymbol{\theta}^T \boldsymbol{\psi}_k + \boldsymbol{\eta}^{*T}\boldsymbol{\varphi}(\boldsymbol{x}_k) + v_k] + |s_{\phi,k}|\rho_\epsilon, \tag{14}$$

where, $\rho_\epsilon = \epsilon_N + \frac{1}{\beta}\epsilon_f(t) + \frac{1}{\beta}|mb_u| \ge |\epsilon(\boldsymbol{x}_k) + \frac{1}{\beta}(f_2(\boldsymbol{x}_k, t) - mb_u)|$.

On the basis of (14), we propose the control law as

$$v_k = -\gamma_1 s_{\phi,k} - \boldsymbol{\theta}_k^T \boldsymbol{\psi}_k - \boldsymbol{\eta}_k^T \boldsymbol{\varphi}(\boldsymbol{x}_k) - \rho_{\epsilon,k}\mathrm{sat}_{-1,1}\left(\frac{s_k(t)}{\phi_k(t)}\right), \tag{15}$$

and learning laws as

$$\boldsymbol{\eta}_k = \mathrm{sat}_{\underline{\eta},\bar{\eta}}(\boldsymbol{\eta}_{k-1}) + \gamma_2 s_{\phi,k}\boldsymbol{\varphi}(\boldsymbol{x}_k), \boldsymbol{\eta}_{-1} = 0, \tag{16}$$

$$\boldsymbol{\theta}_k = \mathrm{sat}_{\underline{\theta},\bar{\theta}}(\boldsymbol{\theta}_{k-1}) + \gamma_3 s_{\phi,k}\boldsymbol{\psi}_k, \boldsymbol{\theta}_{-1} = 0, \tag{17}$$

$$\rho_{\epsilon,k} = \mathrm{sat}_{0,\bar{\rho}}(\rho_{\epsilon,k-1}) + \gamma_4|s_{\phi,k}|, \rho_{\epsilon,-1} = 0, \tag{18}$$

where $\gamma_1 > 0$, $\gamma_2 > 0$, $\gamma_3 > 0$, $\gamma_4 > 0$, $\boldsymbol{\theta}_k$, $\boldsymbol{\eta}_k$ and $\rho_{\epsilon,k}$ are used to approximate $\boldsymbol{\theta}$, $\boldsymbol{\eta}^*$ and ρ_ϵ.

Remark 2: The RBF neural network constructed in (12)-(13) belongs to adaptive learning RBF neural network, which is similar to adaptive RBF neural network [10], [48]. The difference between them lies in: as shown in (17), the former's ideal weight is estimated by using difference learning method, while the latter's ideal weight is estimated by using differential learning method.

Remark 3: In (7), the saturation function $\mathrm{sat}_{\cdot,\cdot}(\cdot)$ is used to construct time-varying boundary layer. In (16)-(18), the saturation functions are adopted for guaranteeing the boundedess of learning variables including $\boldsymbol{\theta}_k$, $\boldsymbol{\eta}_k$ and $\rho_{\epsilon,k}$. More detailed for the explanation on saturation functions, see [26], [45]–[47].

For brevity, in the rest of this paper, $\boldsymbol{\varphi}(\boldsymbol{x}_k)$ is abbreviated as $\boldsymbol{\varphi}_k$, and arguments are sometimes omitted while no confusion occurs.

IV. CONVERGENCE ANALYSIS

We summarize the design in the following statement.

Theorem 1: For the closed loop tank gun servo system (5), control law (15) and learning laws (16)-(18), all system variables are guaranteed to be bounded at each iteration. Moreover, as the iteration number k increases, the closed loop system converges in the sense that

$$\lim_{k\to\infty} s_{\phi,k}(t) = 0, \quad \forall t \in [0, T] \tag{19}$$

and

$$e_{1,k}(t) = \mathrm{e}^{-\lambda t}e_{1,k}(0) + \frac{\mathrm{e}^{-\mu t} - \mathrm{e}^{-\lambda t}}{\lambda - \mu}|s_k(0)|. \tag{20}$$

Proof:

1). Difference of $L_k(t)$

Substituting (15) into (14) leads to

$$\dot{V}_k \le -\gamma_1 s_{\phi,k}^2 + s_{\phi,k}\tilde{\boldsymbol{\theta}}_k^T \boldsymbol{\psi}_k + s_{\phi,k}\tilde{\boldsymbol{\eta}}_k^T \boldsymbol{\varphi}_k + |s_{\phi,k}|\rho_\epsilon - s_{\phi,k}\rho_{\epsilon,k}\mathrm{sat}_{-1,1}\left(\frac{s_k(t)}{\phi_k(t)}\right), \tag{21}$$

where $\tilde{\boldsymbol{\theta}}_k = \boldsymbol{\theta} - \boldsymbol{\theta}_k$, $\tilde{\boldsymbol{\eta}}_k = \boldsymbol{\eta}^* - \boldsymbol{\eta}_k$. Note that $s_{\phi,k}\mathrm{sat}_{-1,1}\left(\frac{s_k(t)}{\phi_k(t)}\right) = |s_{\phi,k}|$. If follows from (21) that

$$\dot{V}_k \le -\gamma_1 s_{\phi,k}^2 + s_{\phi,k}\tilde{\boldsymbol{\theta}}_k^T \boldsymbol{\psi}_k + s_{\phi,k}\tilde{\boldsymbol{\eta}}_k^T \boldsymbol{\varphi}_k + |s_{\phi,k}|\tilde{\rho}_{\epsilon,k}, \tag{22}$$

where $\tilde{\rho}_{\epsilon,k} = \rho_\epsilon - \hat{\rho}_{\epsilon,k}$. Since $V_k(0) = 0$, we deduce from (22) that

$$V_k \le -\gamma_1 \int_0^t s_{\phi,k}^2 d\tau + \int_0^t s_{\phi,k}(\tilde{\boldsymbol{\theta}}_k^T \boldsymbol{\psi}_k + \tilde{\boldsymbol{\eta}}_k^T \boldsymbol{\varphi}_k)d\tau + \int_0^t |s_{\phi,k}|\tilde{\rho}_{\epsilon,k}d\tau. \tag{23}$$

Define a Lyapunov functional as follows:

$$L_k = V_k + \frac{1}{2\gamma_2}\int_0^t \tilde{\boldsymbol{\eta}}_k^T \tilde{\boldsymbol{\eta}}_k d\tau + \frac{1}{2\gamma_3}\int_0^t \tilde{\boldsymbol{\theta}}_k^T \tilde{\boldsymbol{\theta}}_k d\tau + \frac{1}{2\gamma_4}\int_0^t \tilde{\rho}_{\epsilon,k}^2 d\tau. \tag{24}$$

While $k > 0$, on the basis of (23), we can derive

$$L_k - L_{k-1} = -\gamma_1 \int_0^t s_{\phi,k}^2 d\tau - V_{k-1} + \frac{1}{2\gamma_2}\int_0^t (\tilde{\boldsymbol{\eta}}_k^T \tilde{\boldsymbol{\eta}}_k - \tilde{\boldsymbol{\eta}}_{k-1}^T \tilde{\boldsymbol{\eta}}_{k-1})d\tau + \frac{1}{2\gamma_3}\int_0^t (\tilde{\boldsymbol{\theta}}_k^T \tilde{\boldsymbol{\theta}}_k - \tilde{\boldsymbol{\theta}}_{k-1}^T \tilde{\boldsymbol{\theta}}_{k-1})d\tau$$

$$+\frac{1}{2\gamma_4}\int_0^t(\tilde{\rho}_{\epsilon,k}^2-\tilde{\rho}_{\epsilon,k-1}^2)d\tau \tag{25}$$

By using the relationship $(a-b)^2-(a-p)^2\leq a-b)^2-(a-\text{sat}_{\underline{p},\bar{p}}(p))^2$, from (16), we obtain

$$\begin{aligned}&\frac{1}{2\gamma_2}(\tilde{\boldsymbol{\eta}}_k^T\tilde{\boldsymbol{\eta}}_k-\tilde{\boldsymbol{\eta}}_{k-1}^T\tilde{\boldsymbol{\eta}}_{k-1})+s_{\phi,k}\tilde{\boldsymbol{\eta}}_k^T\boldsymbol{\varphi}_k\\&\leq\frac{1}{2\gamma_2}[(\boldsymbol{\eta}^*-\boldsymbol{\eta}_k)^T(\boldsymbol{\eta}^*-\boldsymbol{\eta}_k)-(\boldsymbol{\eta}^*-\text{sat}_{\underline{\eta},\bar{\eta}}(\boldsymbol{\eta}_{k-1}))^T(\boldsymbol{\eta}^*\\&\quad-\text{sat}_{\underline{\eta},\bar{\eta}}(\boldsymbol{\eta}_{k-1}))]+s_{\phi,k}\tilde{\boldsymbol{\eta}}_k^T\boldsymbol{\varphi}_k\\&\leq\frac{1}{2\gamma_2}(2\boldsymbol{\eta}^*-\boldsymbol{\eta}_k-\text{sat}_{\underline{\eta},\bar{\eta}}(\boldsymbol{\eta}_{k-1}))^T(\text{sat}_{\underline{\eta},\bar{\eta}}(\boldsymbol{\eta}_{k-1})-\boldsymbol{\eta}_k)\\&\quad+s_{\phi,k}\tilde{\boldsymbol{\eta}}_k^T\boldsymbol{\varphi}_k\\&\leq\frac{1}{\gamma_2}(\boldsymbol{\eta}^*-\boldsymbol{\eta}_k)^T(\text{sat}_{\underline{\eta},\bar{\eta}}(\boldsymbol{\eta}_{k-1})-\boldsymbol{\eta}_k)+\gamma_2 s_{\phi,k}\boldsymbol{\varphi}_k)\\&=0.\end{aligned} \tag{26}$$

Similarly, from (17) and (18), we can obtain

$$\begin{aligned}&\frac{1}{2\gamma_3}(\tilde{\boldsymbol{\theta}}_k^T\tilde{\boldsymbol{\theta}}_k-\tilde{\boldsymbol{\theta}}_{k-1}^T\tilde{\boldsymbol{\theta}}_{k-1})+s_{\phi,k}\tilde{\boldsymbol{\theta}}_k^T\boldsymbol{\psi}_k\\&\quad\leq\frac{1}{\gamma_3}(\boldsymbol{\theta}-\boldsymbol{\theta}_k)^T(\text{sat}_{\underline{\theta},\bar{\theta}}(\boldsymbol{\theta}_{k-1})-\boldsymbol{\theta}_k)+\gamma_2 s_{\phi,k}\boldsymbol{\psi}_k)\\&\quad=0\end{aligned} \tag{27}$$

and

$$\begin{aligned}&\frac{1}{2\gamma_4}(\tilde{\rho}_{\epsilon,k}^2-\tilde{\rho}_{\epsilon,k-1}^2)+|s_{\phi,k}|\tilde{\rho}_{\epsilon,k}\\&\quad\leq\frac{1}{\gamma_4}(\rho_\epsilon-\rho_{\epsilon,k})(\text{sat}_{0,\bar{\rho}}(\rho_{\epsilon,k-1})-\rho_{\epsilon,k}+\gamma_3|s_{\phi,k}|)\\&\quad=0,\end{aligned} \tag{28}$$

respectively. Substituting (26)-(28) into (25), we have

$$L_k-L_{k-1}\leq-V_{k-1} \tag{29}$$

which further implies

$$L_k(t)\leq L_0(t)-\frac{1}{2\beta}\sum_{j=0}^{k-1}s_{\phi,j}^2. \tag{30}$$

2). Finiteness of $L_0(t)$

By direct calculation, the time derivatives of $L_0=V_0+\frac{1}{2\gamma_2}\int_0^t\tilde{\boldsymbol{\eta}}_0^T\tilde{\boldsymbol{\eta}}_0d\tau+\frac{1}{2\gamma_3}\int_0^t\tilde{\boldsymbol{\theta}}_0^T\tilde{\boldsymbol{\theta}}_0d\tau+\frac{1}{2\gamma_4}\int_0^t\tilde{\rho}_{\epsilon,0}^2d\tau$ may be obtained as

$$\begin{aligned}\dot{L}_0&=-\gamma_1 s_{\phi,0}^2+s_{\phi,0}\tilde{\boldsymbol{\eta}}_0^T\boldsymbol{\varphi}_0+s_{\phi,0}\tilde{\boldsymbol{\theta}}_0^T\boldsymbol{\psi}_0+|s_{\phi,0}|\tilde{\rho}_{\epsilon,0}\\&\quad+\frac{1}{2\gamma_2}\tilde{\boldsymbol{\eta}}_0^T\tilde{\boldsymbol{\eta}}_0+\frac{1}{2\gamma_3}\tilde{\boldsymbol{\theta}}_0^T\tilde{\boldsymbol{\theta}}_0+\frac{1}{2\gamma_4}\tilde{\rho}_{\epsilon,0}^2\\&=-\gamma_1 s_{\phi,0}^2+\frac{\boldsymbol{\eta}_0^T}{\gamma_2}(\boldsymbol{\eta}^*-\boldsymbol{\eta}_0)+\frac{\boldsymbol{\theta}_0^T}{\gamma_3}(\boldsymbol{\theta}-\boldsymbol{\theta}_0)\\&\quad+\frac{1}{\gamma_4}\rho_{\epsilon,0}(\rho_\epsilon-\rho_{\epsilon,0})+\frac{1}{2\gamma_2}(\boldsymbol{\eta}^*-\boldsymbol{\eta}_0)^T(\boldsymbol{\eta}^*-\boldsymbol{\eta}_0)\\&\quad+\frac{1}{2\gamma_3}(\boldsymbol{\theta}-\boldsymbol{\eta}_0)^T(\boldsymbol{\theta}-\boldsymbol{\theta}_0)+\frac{1}{2\gamma_4}(\rho_\epsilon-\rho_{\epsilon,0})^2\\&=-\gamma_1 s_{\phi,0}^2+\frac{1}{2\gamma_2}(\boldsymbol{\eta}^{*T}\boldsymbol{\eta}^*-\boldsymbol{\eta}_0^T\boldsymbol{\eta}_0)\\&\quad+\frac{1}{2\gamma_3}(\boldsymbol{\theta}^T\boldsymbol{\theta}-\boldsymbol{\theta}_0^T\boldsymbol{\theta}_0)+\frac{1}{2\gamma_4}(\rho_\epsilon^2-\rho_{\epsilon,0}^2)\\&\leq-\gamma_1 s_{\phi,0}^2+\frac{1}{2\gamma_2}\boldsymbol{\eta}^{*T}\boldsymbol{\eta}^*+\frac{1}{2\gamma_3}\boldsymbol{\theta}^T\boldsymbol{\theta}+\frac{1}{2\gamma_4}\rho_\epsilon^2.\end{aligned} \tag{31}$$

Since $\frac{1}{2\gamma_2}\boldsymbol{\eta}^{*T}\boldsymbol{\eta}^*+\frac{1}{2\gamma_3}\boldsymbol{\theta}^T\boldsymbol{\theta}+\frac{1}{2\gamma_4}\rho_\epsilon^2$ is bounded, it follows from (31) that $\dot{L}_0(t)$ is bounded for $t\in[0,T]$. As a direct conclusion, we have

$$0\leq L_0(t)<+\infty,\quad\forall t\in[0,T]. \tag{32}$$

3). Convergence of tracking error

Combining (30) with (32), we can draw a conclusion that

$$\lim_{k\to+\infty}s_{\phi,k}(t)=0,\quad\forall t\in[0,T], \tag{33}$$

which means

$$\lim_{k\to+\infty}|s_k(t)|\leq|s_k(0)|\mathrm{e}^{-\mu t},\quad\forall t\in[0,T]. \tag{34}$$

Using the relationship $\dot{e}_{1,k}+\lambda e_{1,k}=s_k$, from (34), we can obtain

$$|e_{1,k}(t)|=\mathrm{e}^{-\lambda t}|e_{1,k}(0)|+\frac{\mathrm{e}^{-\mu t}-\mathrm{e}^{-\lambda t}}{\lambda-\mu}|s_k(0)|. \tag{35}$$

Therefore, $|e_{1,k}(t)|$ decreases exponentially with respect to time since λ and μ are positive. By setting the appropriate value of λ, the closed loop tank gun servo control system may achieve better control performance. ■

In this work, the partial saturation strategy is used to design learning laws for guaranteeing the the boundedness of the estimation of parameters. It effectively improves the security and reliability of controlled systems, comparing with the learning law design of unsaturation strategy.

V. NUMERICAL SIMULATION

Let us consider a tank gun servo system as follows [42]:

$$\begin{cases}\dot{x}_{1,k}=x_{2,k},\\\dot{x}_{2,k}=-\frac{R}{L}x_{2,k}-\frac{K_tK_e}{LJ}x_{1,k}+\frac{K_aK_t}{LJi}u_{q,k}\\\qquad+\Delta f(\boldsymbol{x}_k,t),\end{cases} \tag{36}$$

where $R=0.4\Omega$, $J=5239\text{kg}\cdot\text{m}^2$, $i=1039$, $L=2.907\times10^{-3}$H, $K_t=0.195N\cdot$m/A, $K_e=0.197V/(\text{rad}\cdot s^{-1})$, $B=1.43\times10^{-4}$ N $\cdot$ m, $K_a=2$, $\Delta f(\boldsymbol{x}_k,t)=13.2+0.1x_{1,k}+0.2x_{2,k}+0.2\text{sign}(x_{2,k})+0.2\text{rand1}(k)\sin(0.5t)$, $x_d=0.5\cos(0.5\pi t)$, $T=6$. The system initial state is set as $\boldsymbol{x}_k(0)=[0.3+0.1\text{rand2}(k),0.05\text{rand3}(k)]^T$. Here, rand1($\cdot$), rand2($\cdot$) and rand3($\cdot$) represent random numbers between 0 and 1. The deadzone parameters are $b_r=0.3$, $b_l=-0.4$, $m=1.2$. The control objective is to make $x_{1,k}$ accurately track its reference x_d.

The adaptive ILC law (15) and adaptive learning laws (16)-(18) are adopted in the simulation, with $\gamma_1=10$,

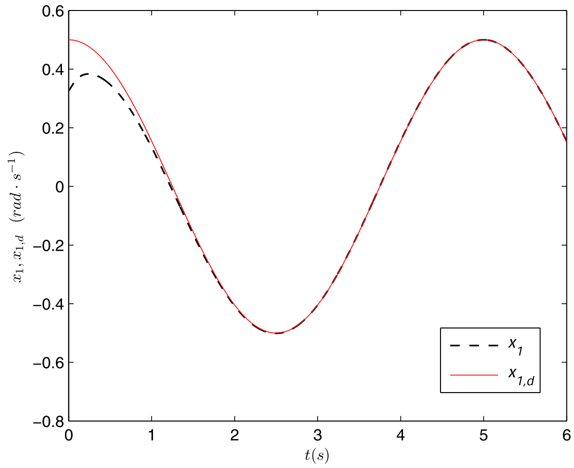

FIGURE 3. x_1 and its reference signal $x_{1,d}$ (TVBL).

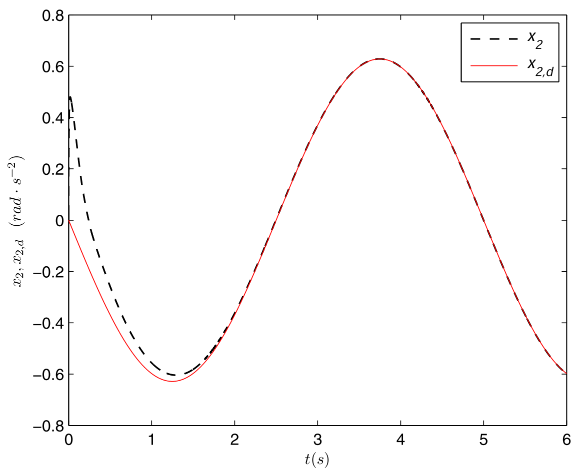

FIGURE 4. x_2 and its reference signal $x_{2,d}$ (TVBL).

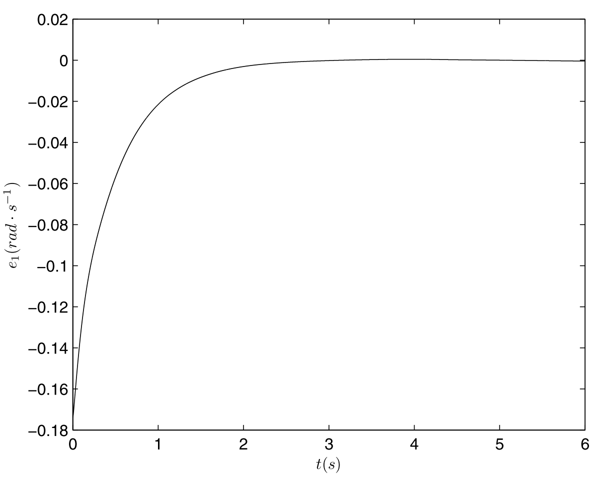

FIGURE 5. The error e_1 (TVBL).

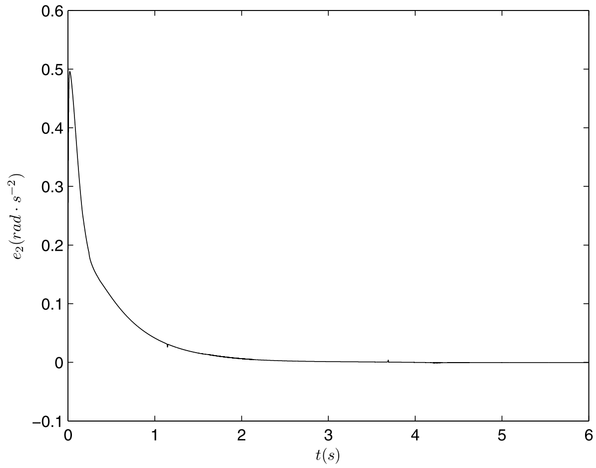

FIGURE 6. The error e_2 (TVBL).

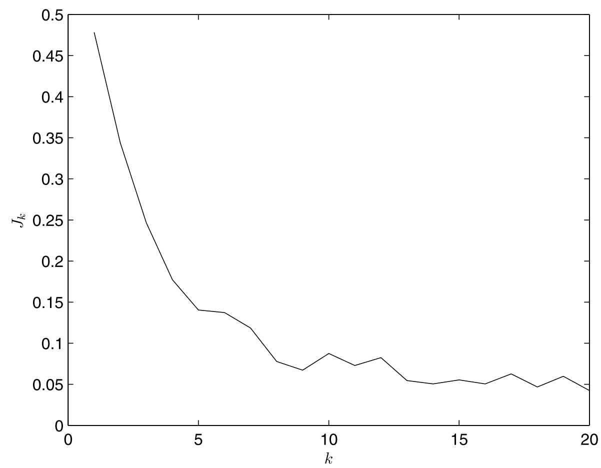

FIGURE 7. Maximum value of $|s_{\phi,k}|$ at each iteration (TVBL).

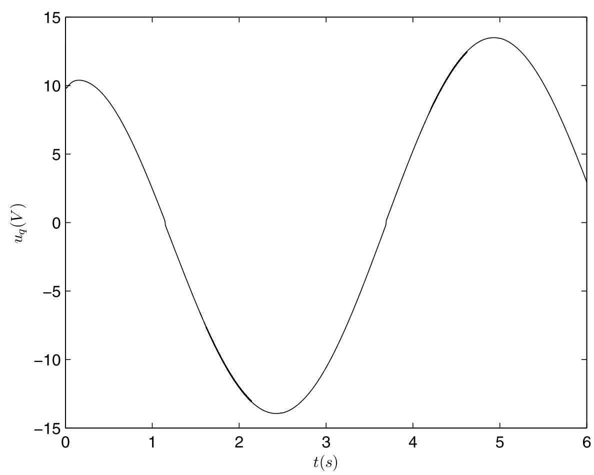

FIGURE 8. Control input (TVBL).

$\gamma_2 = 2$, $\gamma_3 = 2$, $\gamma_4 = 0.02$, $\underline{\theta} = -100$, $\bar{\theta} = 100$, $\underline{\eta} = -30$, $\bar{\eta} = 30$, $\bar{\rho} = 10$. The RBF neural network is constructed as (13), with $b_j = 3$. c_{j1} and c_{j2} are averagely spaced on $[-2, 2]$, for $j = 1, 2, \cdots, 5$. The trajectory-tracking profiles of angular velocity and angular acceleration for the tank gun servo system at the 20th cycle are shown in Figs. 3-4, respectively, with the tracking error profiles illustrated in Fig. 5-6. The convergence history of $|s_{\phi,k}(t)|$ is given in Fig. 7, where J_k is defined as $\max_{t\in[0,T]} |s_{\phi,k}(t)|$. Fig. 8 illustrate the value of control input signal at the 20th iteration. As shown in

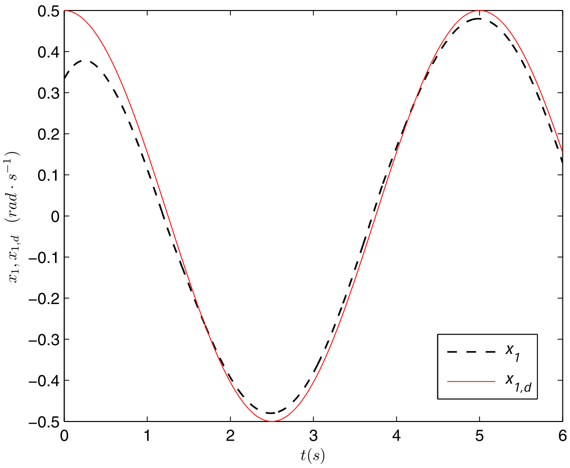

FIGURE 9. x_1 **and its reference signal** $x_{1,d}$ **(TIBL).**

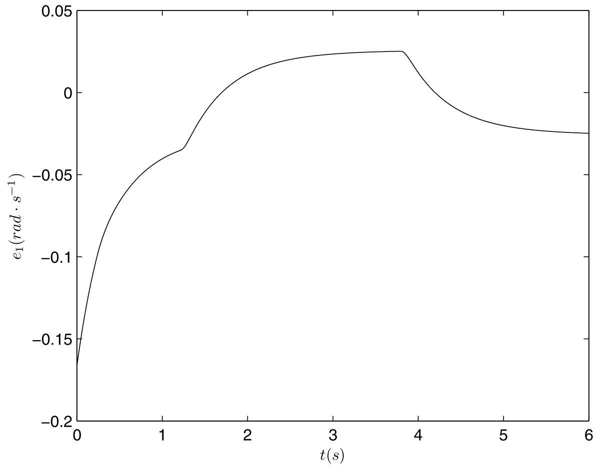

FIGURE 11. **The error** e_1 **(TIBL).**

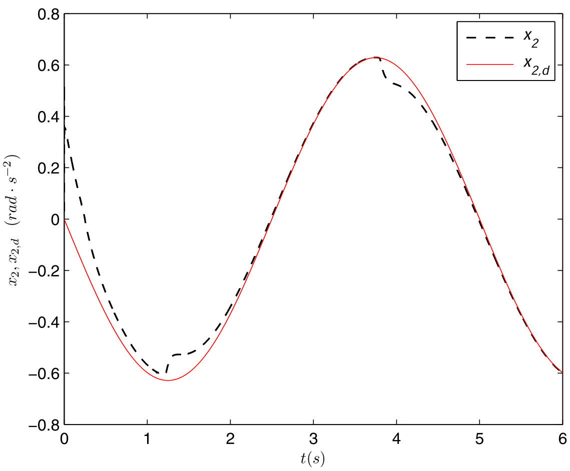

FIGURE 10. x_2 **and its reference signal** $x_{2,d}$ **(TIBL).**

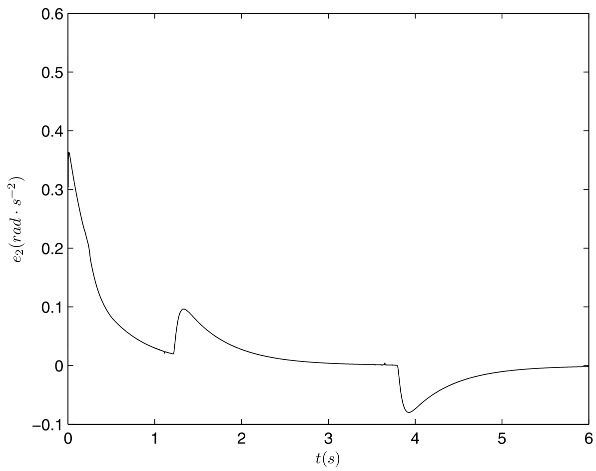

FIGURE 12. **The error** e_2 **(TIBL).**

Figs. 3-7, the closed-loop tank gun servo system owns good tracking performance.

For comparison, the traditional adaptive ILC algorithm (37)-(40) is adopted for simulation. Note that $s_{\varpi,k}$ is different from $s_{\phi,k}$ for ϖ is a time-invariant constant, and $\phi(t)$ is time-varying. That is to say, time-invariant boundary layer (TIBL) applied in (37), which is different from the time-varying boundary layer (TVBL) adopted in (15).

$$v_k = -\gamma_1 s_{\varpi,k} - \boldsymbol{\theta}_k^T \boldsymbol{\psi}_k - \boldsymbol{\eta}_k^T \boldsymbol{\varphi}(\boldsymbol{x}_k) - \rho_{\varpi,k} \mathrm{sat}_{-1,1}\left(\frac{s_k}{\varpi}\right), \tag{37}$$

$$\boldsymbol{\eta}_k = \mathrm{sat}_{\underline{\eta},\bar{\eta}}(\boldsymbol{\eta}_{k-1}) + \gamma_2 s_{\varpi,k} \boldsymbol{\varphi}(\boldsymbol{x}_k), \boldsymbol{\eta}_{-1} = 0, \tag{38}$$

$$\boldsymbol{\theta}_k = \mathrm{sat}_{\underline{\theta},\bar{\theta}}(\boldsymbol{\theta}_{k-1}) + \gamma_3 s_{\varpi,k} \boldsymbol{\psi}_k, \boldsymbol{\theta}_{-1} = 0, \tag{39}$$

$$\rho_{\varpi,k} = \mathrm{sat}_{0,\bar{\rho}}(\rho_{\varpi,k-1}) + \gamma_4 |s_{\phi,k}|, \rho_{\varpi,-1} = 0, \tag{40}$$

where $s_{\varpi,k} = s_k - \varpi \mathrm{sat}_{-1,1}\left(\frac{s_k}{\varpi}\right)$. β is a positive constant and its value is set as 0.02 in this simulation, and other control parameters in (37)-(40) are the same as the ones in the previous simulation. The trajectory-tracking profiles of angular velocity and angular acceleration for the tank gun servo system at the 20th cycle are shown in Figs. 9-10, respectively. The profiles of system error are given in Figs. 11-12, respectively. We can see that system states can not accurately track the corresponding reference trajectories. The maximum value of $|s_{\varpi,k}|$ for 50 cycles is illustrated in Fig. 13, where $J_k \triangleq \max_{t\in[0,T]} |s_{\varpi,k}(t)|$. Comparing Figs. 3-7 with Figs. 9-13, we conclude that it is necessary to handle the nonzero initial errors during the adaptive ILC design for tank gun servo systems, the approach of time-varying boundary layer is useful to solve the nonzero initial error problem for the adaptive ILC development of tank gun servo systems.

The above simulation results verify the effectiveness of the proposed adaptive ILC scheme for tank gun servo systems.

Remark 4: Note that the proposed ILC algorithm is different from finite-time ILC control algorithm [44]. But the control effect, as shown in Figs. 1-4, is similar to that of finite-time ILC control algorithm.

Remark 5: The robust learning control algorithm proposed in [12] is suitable for the tank gun servo systmes whose reference trajectories are smoothly closed. In this work, the above-mentioned assumption is relaxed, which promote the application of ILC technology in tank gun servo systmes. In addition, our proposed algorithm may be used

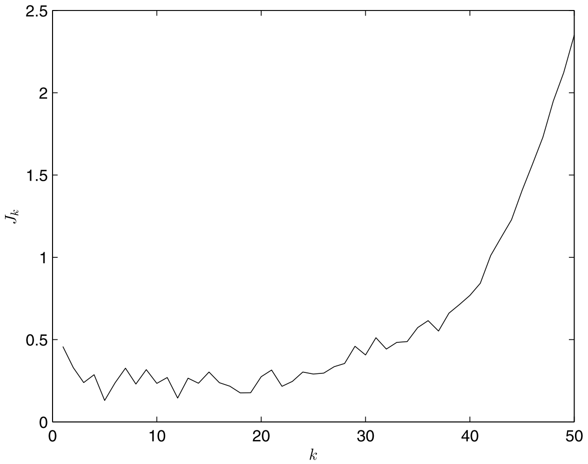

FIGURE 13. Maximum value of $|s_{\varpi,k}|$ at each iteration (TIBL).

in tank gun servo systmes with input deadzone nonlinearity, whereas the algorithm proposed in [12] is suitable to solve trajectory-tracking problem for tank gun servo systmes without input deadzone nonlinearities.

VI. CONCLUSION

The trajectory-tracking problem for tank gun servo systems is addressed in this paper. The iterative learning controller is developed by using Lyapunov approach, with a time-varying boundary layer constructed to deal with the nonzero initial errors. Adaptive learning neural network control and robust control are jointly used to compensate uncertainties and deadzone nonlinearity. According to the simulation result, the closed loop tank gun servo system owns better control performance.

REFERENCES

[1] R. Dana and E. Kreindler, "Variable structure control of a tank gun," in *Proc. 1st IEEE Conf. Control Appl.*, Sep. 1992, pp. 928–933.

[2] W. Grega, "Time-optimal control of n-tank system," in *Proc. IEEE Int. Conf. Control Appl.*, Sep. 1998, pp. 522–526.

[3] S. Shao-Jian, C. Gang, L. Bi-Lian, and L. Xiao-Feng, "Real-time optimal control for three-tank level system via improved ADDHP method," in *Proc. IEEE Int. Conf. Control Automat.*, Dec. 2009, pp. 564–568.

[4] T. Jin, H. S. Yan, and D. X. Li, "PID control for tank firing in motion," *Ind. Control Comput.*, vol. 29, no. 7, pp. 18–19, Jul. 2016.

[5] N. Y. Li, K. C. Li, and Y. L. Liu, "Investigation of direct adaptive controller for tank gun elevation control system," *J. Syst. Simul.*, vol. 23, no. 4, pp. 762–765, 2011.

[6] L. Feng, X.-J. Ma, Z.-F. Yan, and H. Li, "Method of adaptive fuzzy sliding mode control of gun control system of tank," *Electr. Mach. Control*, vol. 11, no. 1, pp. 65–69, 2007.

[7] L.-J. Shen and J. P. Cai, "Adaptive robust control of gun control servo system of tank," *Math. Pract. Theory*, vol. 42, no. 7, pp. 170–175, 2012.

[8] Y. Xia, L. Dai, M. Fu, C. Li, and C. Wang, "Application of active disturbance rejection control in tank gun control system," *J. Franklin Inst.*, vol. 351, no. 4, pp. 2299–2314, Apr. 2014.

[9] J. H. Hu, Y. L. Hou, and Q. Gao, "Sliding-mode control for tank gun controlling system based on disturbance observer," *Electron. Opt. Control*, vol. 25, no. 2, pp. 98–101, 2018.

[10] J. H. Hu, Y. L. Hou, and Q. Gao, "Method of neural network adaptive sliding mode control of gun control system of tank," *Fire Control Command Control*, vol. 43, no. 6, pp. 118–121, 2018.

[11] J. Cai, R. Yu, Q. Yan, C. Mei, B. Wang, and L. Shen, "Event-triggered adaptive control for tank gun control systems," *IEEE Access*, vol. 7, pp. 17517–17523, 2019.

[12] G. Zhu, X. Wu, Q. Yan, and J. Cai, "Robust learning control for tank gun control servo systems under alignment condition," *IEEE Access*, vol. 7, pp. 145524–145531, 2019, doi: 10.1109/ACCESS.2019.2938814.

[13] D. Huang and J.-X. Xu, "Steady-state iterative learning control for a class of nonlinear PDE processes," *J. Process Control*, vol. 21, no. 8, pp. 1155–1163, Sep. 2011.

[14] T. Hu, K. H. Low, L. Shen, and X. Xu, "Effective phase tracking for bioinspired undulations of robotic fish models: A learning control approach," *IEEE/ASME Trans. Mechatronics*, vol. 19, no. 1, pp. 191–200, Feb. 2014.

[15] L. Zhang and S. Liu, "Basis function based adaptive iterative learning control for non-minimum phase systems," *Acta Autom. Sinica*, vol. 40, no. 12, pp. 2716–2725, Dec. 2014.

[16] R. Chi, D. Wang, Z. Hou, and S. Jin, "Data-driven optimal terminal iterative learning control," *J. Process Control*, vol. 22, no. 10, pp. 2026–2037, Dec. 2012.

[17] Y. Q. Wang, E. Dassau, and F. J. Doyle, III, "Closed-loop control of artificial pancreatic β-cell in type 1 diabetes mellitus using model predictive iterative learning control," *IEEE Trans. Biomed. Eng.*, vol. 57, no. 2, pp. 211–219, Feb. 2010.

[18] K. L. Moore, "Iterative learning control: An expository overview," in *Applied and Computational Control, Signals, and Circuits*. Boston, MA, USA: Birkhäuser, 1999, pp. 151–214.

[19] Y. Q. Chen, K. L. Moore, and J. Yu, "Iterative learning control and repetitive control in hard disk drive industry—A tutorial," in *Proc. 45th IEEE Conf. Decis. Control*, Dec. 2006, pp. 2338–2351.

[20] W. Qian, S. K. Panda, and J.-X. Xu, "Torque ripple minimization in PM synchronous motors using iterative learning control," *IEEE Trans. Power Electron.*, vol. 19, no. 2, pp. 272–279, Mar. 2004.

[21] W. Zhang, N. Nan, Y. Yang, W. Zhong, and Y. Chen, "Force ripple compensation in a PMLSM position servo system using periodic adaptive learning control," *ISA Trans.*, vol. 95, pp. 266–277, Dec. 2019.

[22] R.-E. Precup, S. Preitl, I. J. Rudas, M. L. Tomescu, and J. K. Tar, "Design and experiments for a class of fuzzy controlled servo systems," *IEEE/ASME Trans. Mechatronics*, vol. 13, no. 1, pp. 22–35, Feb. 2008.

[23] J.-X. Xu and R. Yan, "On initial conditions in iterative learning control," *IEEE Trans. Autom. Control*, vol. 50, no. 9, pp. 1349–1354, Sep. 2005.

[24] X. E. Ruan and J. Zhao, "Pulse compensated iterative learning control to nonlinear systems with initial state uncertainty," *Control Theory Appl.*, vol. 29, no. 8, pp. 993–1000, 2012.

[25] Q. Z. Yan, M. X. Sun, and H. Li, "Iterative learning control for nonlinear uncertain systems with arbitrary initial state," *Acta Autom. Sinica*, vol. 42, no. 4, pp. 545–555, 2016.

[26] C.-J. Chien, C.-T. Hsu, and C.-Y. Yao, "Fuzzy system-based adaptive iterative learning control for nonlinear plants with initial state errors," *IEEE Trans. Fuzzy Syst.*, vol. 12, no. 5, pp. 724–732, Oct. 2004.

[27] M.-X. Sun and Q.-Z. Yan, "Error tracking of iterative learning control systems," *Acta Autom. Sinica*, vol. 39, no. 3, pp. 251–262, Mar. 2014.

[28] Q. Z. Yan and M. X. Sun, "Error trajectory tracking by robust learning control for nonlinear systems," *Control Theory Appl.*, vol. 30, no. 1, pp. 23–30, 2013.

[29] Q. Z. Yan, M. X. Sun, and H. Li, "Consensus-error-tracking learning control for nonparametric uncertain multi-agent systems," *Control Theory Appl.*, vol. 33, no. 6, pp. 793–799, 2016.

[30] X.-D. Li, M.-M. Lv, and J. K. L. Ho, "Adaptive ILC algorithms of nonlinear continuous systems with non-parametric uncertainties for non-repetitive trajectory tracking," *Int. J. Syst. Sci.*, vol. 47, no. 10, pp. 2279–2289, Jul. 2016.

[31] Q. Z. Yan, M. X. Sun, and J. P. Cai, "Filtering-error rectified iterative learning control for systems with input dead-zone," *Control Theory Appl.*, vol. 34, no. 1, pp. 77–84, 2017.

[32] Q. Z. Yan, M. X. Sun, and J. P. Cai, "Reference-signal rectifying method of iterative learning control," *Acta Autom. Sinica*, vol. 43, no. 8, pp. 1470–1477, Aug. 2017.

[33] D. A. Recker, P. V. Kokotovic, D. Rhode, and J. Winkelman, "Adaptive nonlinear control of systems containing a deadzone," in *Proc. 30th IEEE Conf. Decis. Control*, Dec. 1991, pp. 2111–2115.

[34] G. Tao and P. V. Kokotovic, "Adaptive control of plants with unknown dead-zones," *IEEE Trans. Autom. Control*, vol. 39, no. 1, pp. 59–68, Jan. 1994.

[35] J. Zhou, C. Wen, and Y. Zhang, "Adaptive output control of nonlinear systems with uncertain dead-zone nonlinearity," *IEEE Trans. Autom. Control*, vol. 51, no. 3, pp. 504–511, Mar. 2006.

[36] X.-S. Wang, C.-Y. Su, and H. Hong, "Robust adaptive control of a class of nonlinear systems with unknown dead-zone," *Automatica*, vol. 40, no. 3, pp. 407–413, 2004.
[37] S. Ibrir, W. F. Xie, and C.-Y. Su, "Adaptive tracking of nonlinear systems with non-symmetric dead-zone input," *Automatica*, vol. 43, no. 3, pp. 522–530, Mar. 2007.
[38] W. He, A. O. David, Z. Yin, and C. Sun, "Neural network control of a robotic manipulator with input deadzone and output constraint," *IEEE Trans. Syst., Man, Cybern. Syst.*, vol. 46, no. 6, pp. 759–770, Jun. 2016.
[39] F. L. Lewis, W. K. Tim, L.-Z. Wang, and Z. X. Li, "Deadzone compensation in motion control systems using adaptive fuzzy logic control," *IEEE Trans. Control Syst. Technol.*, vol. 7, no. 6, pp. 731–742, Nov. 1999.
[40] D. Yuan, X. J. Ma, and S. G. Wei, "Direct-transmission drive and dead time compensation control of tank gun control system," *Electr. Mach. Control*, vol. 20, no. 5, pp. 2922–2929, 2016.
[41] J.-J. E. Slotine and W. Li, *Applied Nonlinear Control*. Englewood Cliffs, NJ, USA: Prentice-Hall, 1991.
[42] C. C. Sun, C. Jie, and L. Dou, "Variable structure control for sliding mode of tank stabilizator based on optimization," *Acta Armamentaria*, vol. 1, pp. 15–18, Jan. 2001.
[43] Z. Peng, D. Wang, and J. Wang, "Predictor-based neural dynamic surface control for uncertain nonlinear systems in strict-feedback form," *IEEE Trans. Neural Netw. Learn. Syst.*, vol. 28, no. 9, pp. 2156–2167, Sep. 2017.
[44] M. Sun, "Finite-time iterative learning control," *J. Syst. Sci. Math. Sci.*, vol. 30, no. 6, pp. 733–741, 2010.
[45] W. E. Dixon, E. Zergeroglu, D. M. Dawson, and B. T. Costic, "Repetitive learning control: A Lyapunov-based approach," *IEEE Trans. Syst., Man, Cybern. B. Cybern.*, vol. 32, no. 4, pp. 538–545, Aug. 2002.
[46] X. Jin, S. Lu, J. Qin, and W. X. Zheng, "Auxiliary constrained control of a class of fault-tolerant systems," *IEEE Trans. Syst., Man, Cybern. Syst.*, early access, May 8, 2019, doi: 10.1109/TSMC.2019.2911269.
[47] X. Jin, C. Jiang, J. Qin, and W. X. Zheng, "Robust pinning constrained control and adaptive regulation of coupled Chua's circuit networks," *IEEE Trans. Circuits Syst. I, Reg. Papers*, vol. 66, no. 10, pp. 3928–3940, Oct. 2019.
[48] X. Jin, X. Zhao, J. Yu, X. Wu, and J. Chi, "Adaptive fault-tolerant consensus for a class of leader-following systems using neural network learning strategy," *Neural Netw.*, vol. 121, pp. 474–483, Jan. 2020.

YUNTAO ZHANG received the B.S. and M.S. degrees in computer science from the Zhejiang University of Technology, Hangzhou, in 2002 and 2005, respectively. Since 2005, he has been with the College of Information Engineering, Zhejiang University of Water Resources and Electric Power, where he is currently an Associate Professor. His present research interests are mainly in adaptive control and computer control algorithms.

QIUZHEN YAN received the M.S. degree in computer science from the Zhejiang University of Technology, Hangzhou, China, in 2005, and the Ph.D. degree in control science and engineering from the Zhejiang University of Technology, in 2015. Since 2005, he has been with the College of Information Engineering, Zhejiang University of Water Resources and Electric Power, where he is currently a Lecturer. He is a Senior Member of the Chinese Association of Automation. His present research interests are mainly in iterative learning control and repetitive control.

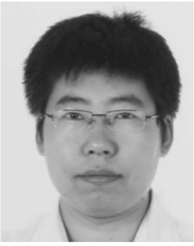

JIANPING CAI was born in 1975. He received the Ph.D. degree from Zhejiang University, in 2014. He is currently an Associate Professor with the Zhejiang University of Water Resources and Electric Power. His main research interests include nonlinear systems and adaptive control.

XIUSHAN WU received the Ph.D. degree in circuit and system from Southeast University, Nanjing, China, in 2009. Since 2009, he has been an Associate Professor with the College of Mechanical and Electrical Engineering, China Jiliang University. He is currently with the School of Electrical Engineering, Zhejiang University of Water Resources and Electric Power. His research interests are dynamic measurement and control, sensing technology, and RF-IC design.